

Effect of point defects on heat capacity of yttria-stabilized zirconia

S. Ostanin¹ and E. Salamatov²

¹*Department of Physics, University of Warwick, Coventry CV4 7AL, UK and*

²*Physico-Technical Institute, Ural Branch of RAS, 132 Kirov Str., 426001 Izhevsk, Russia*

First-principles calculation and anharmonic dynamical theory were used in sequence to explain a large excess heat capacity observed in yttria-stabilized zirconia in comparison with the additive rule value. It is found that the excessive shape of heat capacity decays gradually with the Y_2O_3 doping when the number of environmentally different O sites falls to its zero value at 33 mol % $\text{Y}_2\text{O}_3\text{-ZrO}_2$ due to the Y atoms adjacent. The model and results presented in this work provide a key insight into the complex behaviour and characterization of fast-ion conductors.

PACS numbers: 61.72.-y, 63.70.+h, 65.40.Ba, 85.40.Ry

Point lattice defects both native and artificial, such as vacancies, self-interstitials, solute and substitute atoms, strongly affect the most fundamental properties of materials.[1] In yttria-stabilized zirconia (YSZ), the material with numerous commercial applications [2], formed by the addition of Y_2O_3 to ZrO_2 , the trivalent dopant Y^{3+} substitute for some of the host cations and, in order to maintain charge neutrality, one O vacancy (V_0) must be created for each pair of dopant cations. Y_2O_3 is used to stabilize the tetragonal (*t*) phase of $(\text{ZrO}_2)_{100-x}(\text{Y}_2\text{O}_3)_x$ over the composition range $2 < x < 9$ mol % and the cubic (*c*) fluorite phase with $4 < x < 40$ mol %. The presence of relaxed V_0 and Y substitute atoms make the local atomic environments of YSZ rather different from the stoichiometric high-temperature *t*- and *c*-polymorphs of pure ZrO_2 whose 8-fold cations are distorted and perfectly coordinated, respectively. In YSZ, the average cation coordination number, ranged between 7 and 8, is reduced gradually with increasing Y_2O_3 . If the V_0 associates with Zr ions, as the X-ray absorption findings [3] suggest, it may support a coordination-driven ordering model of stabilization.[4] Placing Y in the next nearest neighbour (NNN) cation positions allows the coordination of Zr in the nearest neighbours (NN) sites to the V_0 to be similar to the monoclinic ZrO_2 arrangement, with Zr located in 7-fold coordination environments, while Y remains 8-fold coordinated.

The electron energy-loss near-edge structure (ELNES) of YSZ demonstrates the features of the experimental O *K*-edge shapes which depend on the crystal structures and the Y_2O_3 composition.[5] In modelling the most important and widely used properties of YSZ the relaxation mechanism is essential. The effects of relaxation were treated within the plane-wave, pseudopotential based free energy molecular dynamics (FEMD) technique.[6] Using the relaxed configurations (RC) of point defects, the ELNES calculations were carried out.[5] Since the results of calculation show very good agreement with the experimental O *K*-edge signal, it seems that theory reflects the realities of relaxation. There is much yet to be learned about the fundamental nature of transport processes in YSZ. Thus, our motivation is to make a contribution to the microscopic modelling and tailoring the

heat capacity of YSZ.

A large excess heat capacity (EHC) has been observed [7] in YSZ at low and room temperatures for 7.8, 9.7 and 11.4 mol % Y_2O_3 compared to the heat capacity calculated from those of pure ZrO_2 and Y_2O_3 by the additivity rule: $\Delta C_p = C_p^{\text{YSZ}} - [(1-x) C_p^{\text{ZrO}_2} + x C_p^{\text{Y}_2\text{O}_3}]$. The shape of $\Delta C_p(T)$ is very similar to that of the Schottky disorder. The same behaviour of heat capacity may yield the two-level system (TLS), quite a simple model, used to simulate the low-temperature properties of amorphous insulators: $C_p^{\text{TLS}} = k_B (\Delta/T)^2 e^{-\Delta/T} / (e^{-\Delta/T} + 1)^2$, where Δ is the energy difference between the levels. C_p^{TLS} shows a maximum at temperature $T_m \simeq 0.42 \Delta$ when the filling-rate variation for the occupied TLS states reaches its maximum value. At $T \gg T_m$, all TLS states are occupied equally and therefore heat capacity decreases as $C_p^{\text{TLS}} \sim 1/T^2$.

It appears that for an anharmonic oscillator (AO), which dynamics is defined by the double-well potential $U(x) = -x^2 + ax^3 + bx^4$, ($a, b > 0$) with a maximum at $x_0 = 0$ and two minima at x_1 and x_2 , separated by the energy $\Delta = U(x_2) - U(x_1) > 0$, the temperature dependence of heat capacity is similar to that of TLS. The partition function $Z_{\text{AO}} = \frac{1}{2\pi\hbar} \int dx dv \exp[-\frac{mv^2/2 + U(x)}{k_B T}]$ is calculated assuming $|U_0| \gg |U_i|$. If U is approximated near its minima by the second-degree polynomials, $U_1 \simeq (x - x_1)^2 \omega_1^2 / 2$ and $U_2 \simeq (x - x_1)^2 \omega_2^2 / 2 + \Delta$ where ω_i are the frequencies of small vibrations at x_i then, using the general thermodynamic relations, one can obtain $C_p^{\text{AO}} = k_B \frac{\Delta^2}{T^2} \frac{\exp(-\Delta/T)}{\exp(-\Delta/T + \omega_1/\omega_2)^2} + k_B$. In the latter, the temperature dependence of the first term, $\Delta C(T)$, which defines the difference in heat capacity between anharmonic and harmonic oscillators, is close to C_p^{TLM} and finally, at $\omega_1/\omega_2 = 1$, $\Delta C \equiv C_p^{\text{TLM}}$. Hence, the EHC effect may appear as the result of strong anharmonic vibration modes either localized or delocalized ones.

The fact that at $x > 8$ mol % Y_2O_3 ΔC_p decreases [7] with increasing the dopant concentration may suggest that the delocalized anharmonic vibrations cause the EHC effect. It is known that the main contribution to the structural transformations comes from particular vibrational modes. In pure ZrO_2 , a zone-boundary soft phonon, X_2^- , which breaks the *c*-symmetry of the O sub-

lattice, displacing the O atoms toward their positions in the t -phase, may be responsible for the $c-t$ phase transformation. In YSZ, the experimental data [8] are not fully clarified for this soft mode because of the static disorder in the O sublattice. Using the RC of YSZ, the X_2^- -like phonon was calculated [9] by means of the frozen-phonon method for each composition of $(\text{ZrO}_2)_{100-x}(\text{Y}_2\text{O}_3)_x$ between 3 and 10 mol % Y_2O_3 . For 10 mol % Y_2O_3 , the effective potential has a single minimum and, with decreasing Y_2O_3 content, the potential develops two minima. The temperature dependence of the phonon frequency, calculated within the modified pseudoharmonic approximation, quantifies accurately the transition temperature above which the c -phase is stabilized.[9] In the 3 mol % Y_2O_3 case, it may start around room temperature. The upper boundary of the single t -phase field in the experimental phase diagram [10] shows a similar rapid drop of temperature with Y_2O_3 concentration. However, the X_2^- -like soft phonon of YSZ, in another words, the delocalized vibrations can not be responsible for the EHC effect because of the potential symmetry.

Regarding anharmonic effects, the atomic vibrations localized near the V_0 should be considered as well. YSZ is a solid electrolyte in which ionic transport takes place by anions moving among their positions by the vacancy diffusion mechanism. If any two V_0 sites, which an O atom occupies before and after a diffusive jump, are non-equivalent then theory enables the double-well asymmetric potential profile. In such a study of diffusion, the molecular dynamics technique can fruitfully be used. The principal output of the dynamic computation is the set of atomic trajectories from which all other properties are calculated. Molecular dynamics has been used in the past by many authors to calculate the potential energy dependant on the position of diffusion atom.[1] Even if one could calculate the induced trajectories through the saddle-point the results were strongly affected by the reaction coordinates of all other atoms. The benefits and limitations of this molecular dynamics approach have been discussed and it is generally accepted now that using the large unit cells this scheme is very complicated for precise calculation whereas the results, obtained in such a way, are not always satisfactory.[11]

The features of the computed U profile were demonstrated using the single- V_0 11-atom $\text{Zr}_2\text{Y}_2\text{O}_7$ cell, which contains two formula units of ZrO_2 and one formula unit of Y_2O_3 , that corresponds to a composition of 33 mol % Y_2O_3 . [12] The RC, shown in the (a) panel of Fig. 1, was used in a further static optimization using the displacements of O-2 along the z -direction while all other atoms are fixed at their relaxed positions. In this case, labeled in the panel (b) of Fig. 1 as a “solid pass” trajectory, the O-2 position in the $z=0$ plane corresponds to the saddle point with the potential barrier E_b of ~ 0.2 eV/cell. If Zr in the $z=0$ plane were allowed to relax when the O-2 is moved, as shown in Fig. 1 as the “soft pass” trajectory, then the equilibrium position of O-2 is much closer to the saddle point while E_b becomes significantly

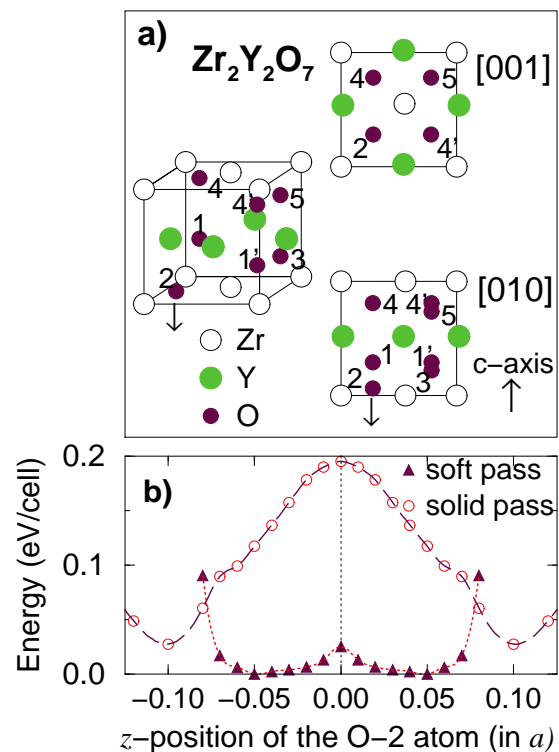


FIG. 1: Model of $\text{Zr}_2\text{Y}_2\text{O}_7$ after relaxation is shown in the (a) panel. The plan views shown in (a) represent the views along the [001] and [010] directions. The O-2 displacement along [001] is marked by an arrow. In the (b) panel, the curve, labelled as solid pass, shows the change in the FEMD energy as a single O-2 atom is moved from its equilibrium position along the z axis while all other atoms are fixed at their relaxed positions. The soft-pass curve, shown after shifting to a common zero energy, corresponds to the O-2 displacements when its nearest Zr may relax.

less. In $\text{Zr}_2\text{Y}_2\text{O}_7$, where all O sites are equivalent to each other, the Zr/Y environment enables the symmetric form of $U(x)$ and therefore can not result in the EHC effect. The saddle-point neighborhood plays a key role on the instability-barrier formation, which is very sensitive to the model parameters. Thus, the dynamics theory of ion transport is still very much a semiempirical science and further simplification, based on the realities for the activation energy, should be made.

Atomistic RC of the $(96-y)$ -atom supercells ($y=1,2,\dots$) allow to model $(\text{ZrO}_2)_{100-x}(\text{Y}_2\text{O}_3)_x$. In the 95-atom cell, which corresponds to ~ 3 mol % Y_2O_3 , the RC with both Y atoms in the NNN shell was obtained.[5] Fig. 2 shows the RC energies, expressed as an equivalent temperature per 12-atom cell, to give an idea of the relative stability and temperature required. In the 94-atom cell, the RC with two V_0 s along the $\langle 111 \rangle$ fluorite direction results in a 6-fold coordinated and six 7-fold coordinated NN Zr atoms. This result supports the interpretation of the neutron data by Goff et al. [14]. Electrostatic considerations suggest that V_0 s should repel. From this point of

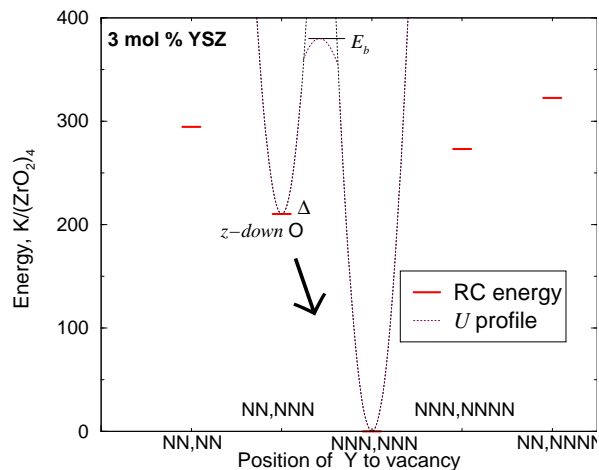


FIG. 2: Relaxed energies of the 95-atom YSZ cell are plotted vs positions of the two Y dopant cations on the NN or/and NNN cation shells. The diffusion jump of the lower apical NN O allows to construct the double-levels potential U shown in the diagram as a sketch.

view, the tri- V_0 RC, with all V_0 separated by $\sqrt{5}/2$ from each other (in units of the c - ZrO_2 lattice constant a), is rather reasonable. The repulsion tendencies between vacancies consistent with both electrostatics and the Zr-coordination lowering model. Since the shortest distance of $a/2$ between the V_0 sites is not energetically favorable in YSZ at low Y_2O_3 concentrations we believe that each V_0 has six NN O atoms each of which can jump into the empty site.

The intrinsic process of such chaotic O moves should occur in YSZ at finite temperatures via the vacancy mechanism. In particular, when an apical O in 3 mol % Y_2O_3 moves into V_0 the RC with the Y NN and NNN atoms is created. The difference $\Delta=210$ K between these two RC was used to construct the potential profile, as shown in the lower diagram of Fig. 2. If V_0 moves consequently into the next O site of this anion tunnel along the z axis, the Y NN-NNNN configuration is realized. We take $E_b = E_a \approx 1$ eV using the activation energy E_a of YSZ, obtained from the Arrhenius relation for the ionic dc conductivity [13] $\sigma \sim \omega_0 d^2 \exp(-E_a/k_B T)$, where ω_0 is the attempt frequency. To form the effective potential, characterized by E_b , Δ and the distance moved during a single jump $d=|x_1 - x_2|$, the three-parameter polynomial $U(x) = -ax^2 + bx^3 + cx^4$ was used. Since $E_b \gg \Delta$, the O vibrations near the U minima may be estimated as $\omega \approx \sqrt{\frac{32E_b}{md^2}}$, where m is the O mass. As a result, $\omega \approx 5 \times 10^{14}$ Hz is close to that found experimentally [15] showing very reasonable model approximation.

In Fig. 3a the calculated EHC shape $\Delta C_p(T) = \mathcal{N}^{TLS}$. C_p^{TLS} is plotted, with its dependence on temperature and dopant concentration. Here \mathcal{N}^{TLS} was obtained in such a way that each maximum coincides with the experimental EHC amount [7] at 7.76, 9.7 and 11.3 mol %

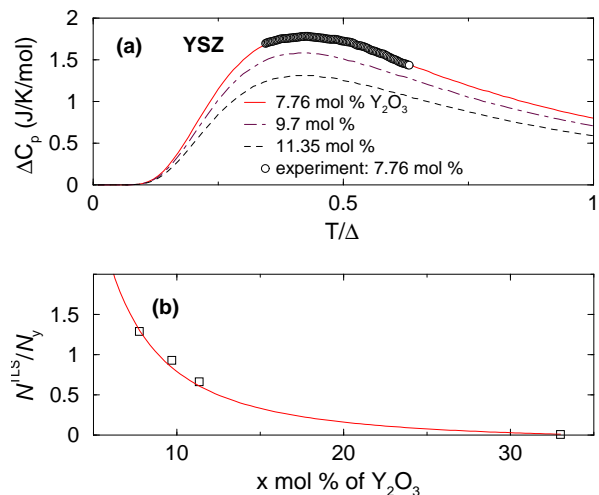


FIG. 3: Calculated ΔC_p for the 7.76, 9.7 and 11.35 mol % Y_2O_3 - ZrO_2 are shown vs T/Δ in the (a) panel compared with the experimental EHC shape of 7.76 mol % Y_2O_3 . In the panel (b), the ratio of \mathcal{N}^{TLS} , obtained using ΔC_p , to the number of vacancies N_y are shown as \square for each Y_2O_3 concentration and connected by eye.

Y_2O_3 . The EHC observations of 7.76 mol % Y_2O_3 are shown in Fig. 3a to illustrate the similarity. All theoretical ΔC_p shapes, with a maximum at 88 K, have been aligned with the experimental peak at $T_m=75$ K using the T/Δ dimensionless scale. The (b) panel of Fig. 3 shows that the \mathcal{N}^{TLS}/N_y ratio (N_y is the number of V_0) falls quickly with increase in Y_2O_3 content and, finally, $\mathcal{N}^{TLS}/N_y \rightarrow 0$ at $x=33$ mol % when the U symmetry for diffusion atom should appear. At low concentrations of Y_2O_3 , not all possible diffusion jumps lead to the asymmetric U . For example, in 3 mol % Y_2O_3 , $N_y=1$ whereas \mathcal{N}^{TLS} falls from six to four since two O NN sites to V_0 are energetically equivalent due to the Y atoms adjacent. The number of such environmentally equivalent O sites, which not contribute to the EHC effect, increases with increasing the dopant concentration.

The high-probability O hopping via V_0 between the low-energy equivalent sites, localized close up to each other, can be considered as some sort of the vacancy block, which results in the anisotropic absorption peak to the internal frictions measured in 9.5 mol % Y_2O_3 . [15] This observation is in agreement with our findings confirming earlier suggestions that some vacancies exist in bound states as di- V_0 along the [111] fluorite direction. As the number of V_0 -blocks increases with Y_2O_3 doping, the peak magnitude for the localized relaxation may not scale simply with the dopant concentration, reaching a maximum at some critical concentration x_m correlated with that of the EHC maximum. At $x > x_m$, the number of sites on the O sublattice with similar local environment increases significantly. This may lead to the long-range transport of O ions via vacancies reducing therefore the local hopping process in V_0 -blocks. Regarding the con-

centration profile of localized relaxation explained, such observations at $x > x_m$ may be masked by overlap between the isotropic and anisotropic absorption peaks due to diffusion and V_0 -block relaxation, respectively.

In *summary*, our study of YSZ being performed using the *ab initio* relaxed configurations and dynamical model of O hopping allows to explain the EHC anomaly observed with the Y_2O_3 doping. In YSZ, as it has been demonstrated, the anisotropic absorption peak of internal frictions and EHC effect have a common vacancy-

block nature showing great potential for theory to deal with the realistic model of doped ceramics. Because of the general physics involved we believe that similar excessive behaviour of heat capacity might be observed in a wide class of ionic conductors where anion hopping goes through non-equivalent positions.

E.S. thanks Russian Basic Research Foundation (Grants No. 00-02-17426, 01-02-96462) for financial support.

-
- [1] C.P. Flynn, *Point Defects and Diffusion*, (Clarendon Press, Oxford, 1972), p. 423.
- [2] E. C. Subbarao, in *Science and Technology of Zirconia*, edited by A. H. Heuer and L. W. Hobbs, *Advances in Ceramics*, Vol. 3 (American Ceramic Society, OH, 1981).
- [3] P. Li *et al.*, Phys. Rev. B **48**, 10063 (1993).
- [4] E.V. Stefanovich *et al.*, Phys. Rev. B **49**, 11560 (1994).
- [5] S. Ostanin *et al.*, Phys. Rev. B **65**, 224109 (2002).
- [6] A. Alavi *et al.*, Phys. Rev. Lett. **73**, 2599 (1994).
- [7] T. Tojo *et al.*, J. Thermal Analysis Calorimetry **57**, 447 (1999).
- [8] D.W. Liu *et al.*, Phys. Rev. B **36**, 9212 (1987); D.N. Argyriou and M.M. Elcombe, J. Phys. Chem. Solids **57**, 343 (1996).
- [9] S. Ostanin *et al.*, Phys. Rev. B **66**, 132105 (2002).
- [10] R.A. Miller *et al.*, in *Science and Technology of Zirconia*, edited by A. H. Heuer and L. W. Hobbs, *Advances in Ceramics*, Vol. 3, (American Ceramic Society, OH, 1981).
- [11] C.H. Bennett, in *Diffusion in solids. Recent developments*, edited by A.S. Nowick and J.J. Burton, (Academic Press, NY, 1975).
- [12] S. Ostanin *et al.*, Phys. Rev. B **62**, 14728 (2000).
- [13] A. Cheikh *et al.*, J. Europ. Ceram. Soc. **21**, 1837 (2001).
- [14] J.P. Goff *et al.*, Phys. Rev. B **59**, 14202 (1999).
- [15] M. Ohta *et al.*, Physica B **316-317**, 427 (2002); M. Ohta *et al.*, Phys. Rev. B **65**, 174108 (2002).